SAND2022-0734C

Wake state estimation of downwind turbines using recurrent neural networks for inverse dynamics modelling

W Farrell[1], T Herges[1], D Maniaci[1] and K Brown[1]

[1]Sandia National Laboratories, Albuquerque, NM, 87185, United States of America

Email: wfarrel@sandia.gov

Abstract. Presented in this work is a novel approach to estimate absolute lateral wake center position on the rotor plane of a waked turbine using turbine load and operating state information. The approach formulates the estimation of the absolute lateral wake position as an inverse dynamics problem and utilizes a recurrent neural network to model the inverse mapping between the wake center position and select turbine output channels. The technique is validated on experimental data collected from experiments at the Sandia Wind Farm Technology (SWiFT) facility and numerical simulations of the site in the wind farm simulator FAST.Farm. Estimator performance and analysis of optimal conditions for estimation are discussed as well as potential control system design opportunities using the estimation technique.

1. Introduction

The waking of downstream turbines within a wind farm is a well-known and unavoidable phenomenon which in most contexts possesses negative consequences in terms of downstream turbine loading and power production [1]. Therefore, of great benefit for a controls engineer would be information of the impinging wake center position on a downstream turbine. Such information would aid in the development of currently active areas of wind farm control such as axial induction control and wake steering as well as aid in the development of novel controllers for optimal downstream turbine operation in waked states.

Current approaches for estimating impinging wake center positions typically require lidar systems which are both complex and costly [2]. In addition to these approaches model-based approaches such as those presented in [3] can be used to categorize wake center positions as either being on the left or right side of the rotor plane. This model-based approach however does not showcase the capability of estimating a quantitative value for the absolute wake center position. This work presents a new methodology whereby the downstream turbine is used as a sensor to detect the location of the wake center of an impinging wake acting on its rotor plane. The benefit of such an approach will be its ease of implementation on existing wind turbine systems as well as its low cost. The approach will be made by inverting the dynamic relationship between easily obtainable turbine outputs and inputs. Additionally, the development of the inverse system will be done using a data driven recurrent neural network approach (RNN).

2. Objectives

The overall objective of this work is to develop a methodology which will allow for the fast estimation of an impinging wake center position on a downstream wind turbine suitable for iterative control system

design. This overall objective is subsequently broken down into two components. The first component is the determination of easily obtainable I/O data from the downstream turbine which possess strong dynamic coupling. Restricting the data channels to easily obtainable metrics allows for greater utilization of the methodology on existing wind farms with waked wind turbines. Additionally, the dynamic coupling requirement will prove to be necessary in maximizing the inverse model training performance.

The second component is on the development and training of a RNN for the modelling of the inverse dynamics of the wind turbine system. For reasons which will be explained in Section 3.2, RNNs provide a framework with features very useful for dynamic system modelling and have therefore been chosen to model the inverse dynamics of our system. Be that as it may, various application dependent hyperparameters (I/O delays, number of neurons/layers, activation functions, etc…) must be determined to fully take advantage of the benefits provided by the RNN framework.

3. Methodology

3.1 Forward and Inverse Dynamic System Framework

The development of the inverse dynamic model used in the present waked position estimation technique begins with defining a forward dynamic model of a single wind turbine. The definition of this forward model takes the form

$$y(k) = F(y(k-1), .., y(k-n), u(k-d), \dots, u(k-d-m) \tag{1}$$

where k is the current time index, $\boldsymbol{y}$ is a vector of output channels, $\boldsymbol{u}$ is a vector of input channels, the function F represents a nonlinear mapping of the input states to the output states, and variables d, n, and m represent the delay between the input and output states and the respective windows in which previous outputs and inputs influence the current output respectively. The selected inputs and outputs for the system model must be data channels with strongly coupled dynamics. In this vein and with the intention of making an inverse model, the input channel used in this work is the absolute wake center lateral deviation from the downstream rotor center. The output channels chosen are the rotor rpm, flap-wise blade root bending moment, and the generator torque. These output channels are chosen due to the strong influence of the wake motion on these channels, which is based on the physical connection between the inflow distribution and resulting rotor torque generation and subsequent generator torque controller response. Additionally, with the possible exception of the flap-wise blade root bending moment, these outputs are readily available on most commercial turbines.

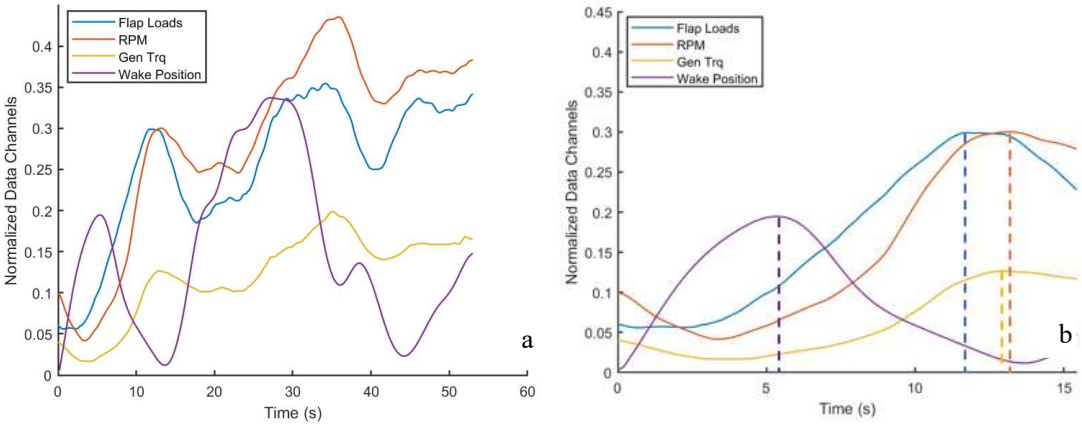

Figure 1: Example normalized I/O data channels (flap-wise root bending moment, rotor rpm, generator torque, and lateral wake position) (a) and up-close view of I/O time series delays (b) for inverse model.

Using the defined forward model, the inverse model which will allow for the estimation of the absolute lateral deviation of the wake center is defined as

$$u(k) = G(y(k+d)..y(k+d-n), u(k-1) \dots u(k-m)) \tag{2}$$

where all variables are defined from the forward model definition and the new function G is the inverse mapping of the input space to output space. The nonlinear inverse function G is particularly difficult to determine if it is not possible to define it analytically using first principles due to the complex nonlinear nature of the forward process. To circumvent this issue a RNN is employed to model the inverse dynamics function and will be discussed in Section 3.2.

In Figure 1 an example normalized I/O data bin is shown for the inverse model. To achieve better correlation between the flap-wise blade root bending moment and the absolute wake center position a moving average process is applied to the data channel in both the forward and backwards direction. Averaging is needed only for the flap-wise blade root bending moment as it possesses high frequency oscillations that far exceeds the oscillation frequencies seen in the other outputs as well as the input. It is observed that the response of the output channels lags the input channel by a significant margin. The lags between the wake position motion and the generator torque and rotor rpm are nearly identical, which is a result of the fast response of the rotor rpm with respect to changes in the generator torque. The primary drivers of the significant lag between the wake position and generator torque can be decomposed into two main contributors. The first of these drivers is the relative insensitivity of the rotor effective wind speed to wake position motions when the wake position is close to the rotor center which results in a delay in the generator torque response. The second driver is the relatively slow dynamic response of the generator torque controller with respect to changes in the rotor effective wind speed. The lag between the wake position motion and the averaged flap-wise bending loads is by comparison shorter in duration. This observation can be considered intuitively as wake center motions have a near immediate influence on blade loads and therefore influences the averaged blade load channel quicker than the other two channels. In the context of this work these observations help in determining the *d*, *n*, *m* variables in the forward and inverse model definitions.

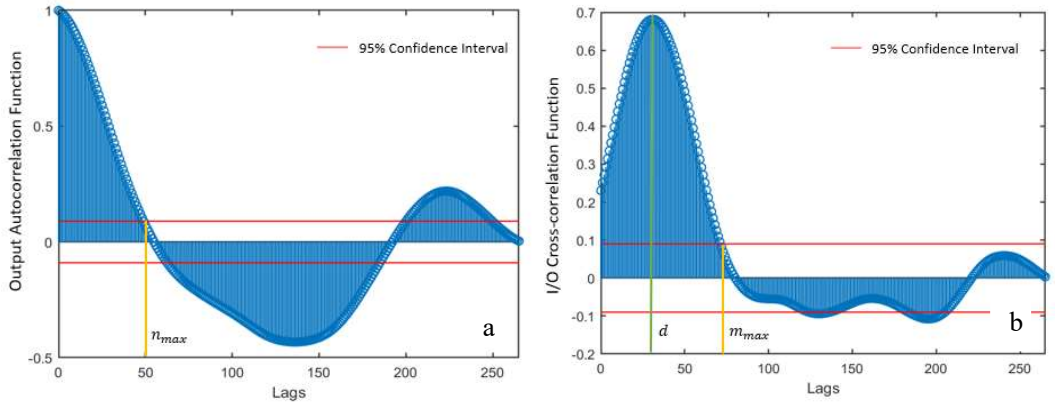

Figure 2: Example forward model autocorrelation (a) and cross-correlation functions (b) using absolute lateral wake center position and generator torque channels

The determination of the model parameters *d*, *n*, and *m* is of high importance as these parameters dictate the portions of the I/O timeseries that will be used in the model inversion process at each time step. Therefore, a necessary step in this work is to determine these parameters such that the selected timeseries portions provide maximal information for neural network training. Parameter determination begins with computing relevant autocorrelation and cross correlation functions for the forward model I/O timeseries.

It should be noted the parameters *d*, *n*, and *m* are not constant over all waked conditions and therefore could benefit from being optimized for specific waking conditions. This is not considered in this study.

By computing the cross-correlation between the inputs and outputs of the forward model the parameter *d* is determined as the lag with the highest correlation. The parameter *m* is the difference between the lag associated with parameter *d* and the lag at which the correlations no longer meet a pre-determined correlation threshold. The parameter *n* is determined from the autocorrelation function of the forward model outputs and is the last lag at which the correlations meet a pre-determined correlation threshold. An intuitive threshold for parameter determination is the expected autocorrelation coefficient that exceeds 95% of all other autocorrelation coefficients in magnitude that are derived from timeseries taken from a normal distribution. These time series are equivalent in length to the I/O data channels. In Figure 2, these parameters are plotted on example autocorrelation and cross-correlation functions. Obtaining parameters *n*, and *m* in this manner provides the largest amount of data per forward model function evaluation but in practice, model overfitting as well as slow model training may occur. Therefore, the parameters *n* and *m* should be kept as small as possible and increased until a desired level of model performance is achieved. Using this information, a brute force evaluation of the estimator performance using a variety of *n*, and *m* values and the value of *d* as determined from the cross-correlation analysis is conducted. Of the three possible I/O relationships available to determine these parameters, the generator torque and wake center position combination is arbitrarily used in this work. Through this process *d*, *n*, and *m* values of 25, 15, and 5 are obtained.

3.2 RNN Overview and Training Procedure

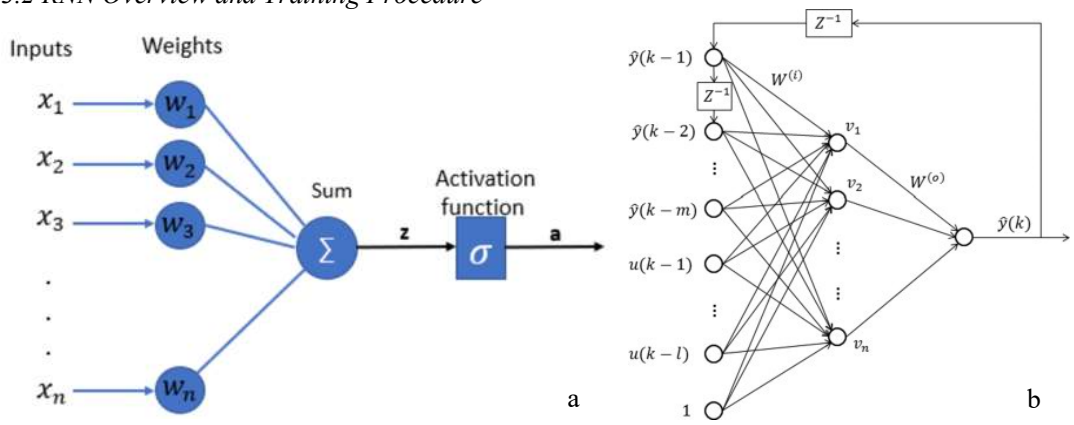

Figure 3: Diagram of perceptron adapted from [4] (a) and nonlinear autoregressive with exogenous inputs (NARX) RNN framework adapted from [5] (b)

RNNs are a class of neural networks in which the outputs of the network are directly fed back into the network and used in the determination of the next output. Figure 3 shows diagrams of a traditional perceptron and a nonlinear autoregressive with exogenous inputs (NARX) recurrent network framework. The diagram of the perceptron can be interpreted as a closer look at the computations that occur at each neuron in the hidden layer of the NARX RNN framework. This framework makes it especially useful in modelling dynamic systems due to its inherent memory retention which is also present in the coupled I/O data of dynamic systems. In the context of this work a coupled data set of rotor rpm, flap-wise blade bending load, and generator power responses that will be described in Sections 3.3 and 3.4 are used as inputs in the RNN training while the absolute lateral deviation of the wake position is used as the output. The RNN inverse model is trained using batches of data simultaneously to improve robustness of wake position estimator. The training is performed using a Levenberg-Marquardt nonlinear optimization routine [6] which minimizes the mean squared error

between the close-loop RNN outputs, and the training dataset outputs. To further improve robustness this process is repeated on 100 RNNs in which the outputs of the 5-best performing RNNs are averaged to produce a final wake position estimator. Current values of the RNN hyperparameters were selected through a preliminary architecture search. The presented results are obtained using single layer RNNs with log-sigmoid hidden layer activation functions and 5 neurons per layer.

3.3 Experimental Acquisition of I/O Data

The described methodology is tested on data taken from waked wind turbine experiments conducted at the Sandia Wind Farm Technology (SWiFT) facility [7]. In these experiments the wake position and wake velocity distribution on the downwind turbine were measured using a custom built DTU SpinnerLidar system [2] focused 5 rotor diameters downwind of the leading turbine on which the lidar system was mounted. Rotor rpm and generator torque measurements were obtained directly from the turbines onboard data collection system while the flap-wise blade loads were derived from strain measurements using a collection of fiber-bragg grating strain sensors at the blade root [8]. Values for external variables not directly accounted for in the estimation technique such as free stream wind speed and turbulence intensity ranged from 5-10 m/s and 4.5% -11% respectively.

The data channels collected in this experiment were sampled at a variety of rates. Of the selected I/O data from this experiment, the lidar wake position measurements were sampled at a maximum frequency of 0.5 Hz and all other channels are sampled at 50 Hz. Due to the large variation in sampling frequencies, all data is resampled to 5 Hz. A cubic spline interpolation is used to provide smooth variation of the wake position particularly in the places where there are small gaps in the wake position data. As referenced in Section 3.1, the flap-wise blade root bending moment is averaged using a 2-second moving average window.

3.4 Medium-Fidelity Semi-Empirical Wind Farm Modelling for I/O Data

In addition to testing this methodology on experimental data an identical study is conducted using the medium fidelity wind farm simulator FAST.Farm [9]. The simulator FAST.Farm leverages the models developed in the aero-elastic turbine simulator OpenFast for the modelling of individual turbines while additionally modelling ambient flow field effects on the resulting turbine wakes and the effects of wakes on downstream turbines using the dynamic wake meandering (DWM) model. Validation of the simulator against high-fidelity Large-Eddy Simulations (LES) was conducted in [10] for the NREL 5 MW reference wind turbine. In the presented study the SWiFT V27 turbines are modelled, which gives one source of model uncertainty as the DWM model has not been re-tuned specifically for this turbine. The OpenFast models of the V27 turbine are validated against experimental results in [11] and compared against various high-fidelity models in [12]. For this study, turbine nacelle and tower dynamics are modelled, however active turbine yawing and blade pitching during a simulation are not considered.

The flow fields used in the simulation environment are obtained using the turbulent flow field generator TurbSim [13]. As TurbSim outputs planar flow field data, the vertical and horizontal directions are discretized to a resolution of 1 meter and a time step size of .005 s is used. These turbulent flow fields correspond with a neutral boundary layer, and mean wind speeds of 6.7 and 8.7 m/s at hub height corresponding to conditions typically seen at the SWIFT site [11]. Turbulence is modelled using the Kaimal turbulence model in conjunction with an exponential coherence model using best practice coherence parameters found in [9]. Turbulent intensities of 12.6% for the 6.7 m/s cases as well as 6% and 10.8% for the 8.7 m/s cases are used. Using a power law model for the atmospheric boundary layer, a shear exponent of 0.14 and veer rate of 0 °/m is used for all cases. It is important to note that 10 minutes of flow field data using the aforementioned settings required 8 days to complete due to TurbSim's inability to take advantage of parallel computing resources. Alternative approaches could include other

semi-empirical turbulence models or to use LES flow fields that would potentially require less time, although with far greater computational resource requirements.

4. Results

4.1 Validation on Experimental Data

Using experimental data binned in 47 second intervals, 68 bins of data were used in the parallel RNN training process. A leave-out set of 18 bins is used to validate the performance of the methodology. A 5-fold cross validation is performed using the full dataset to reduce the effect of variations in training and validation case partitioning on the final estimator performance. Examples of performance over two different bins are showcased in Figure 4 where the wake position estimates are nondimensionalized by the rotor diameter. The performance of the wake position estimator is strong with respect to matching the amplitude and phase of the absolute wake center deviation dynamics. This strong performance was observed over most of the validation cases used in the study. The result of the 5-fold cross validation is a median root-mean-square error (RMSE) in wake position estimation of 3.562 m. This metric converts to a nondimensional RMSE of 0.132 with respect to the rotor diameter and further showcases the accuracy of this method.

By analyzing the underperforming data bins from the cross-validation routine, turbine operating scenarios which prove difficult for the estimator are determined. An example of a bin which saw lower estimator performance is shown in Figure 4b. In situations where there is relatively constant or slow-moving wake positions and system inputs, a significant bias between the estimated wake center position and the true wake center position can develop. In such scenarios however, the overall dynamics of the wake position time history can still be well estimated. This issue is most likely related to the RNN model weighting more heavily the coupled dynamics of its input as opposed to the raw values of the data channels. Additionally, it is observed that the technique has difficulty in estimating the wake position when the wake is near the center of the rotor plane. This difficulty in estimation is a result of the relative insensitivity of the data channels to wake position motions when the turbine is in a near full to fully waked condition. In these conditions the movement of the wake predominately influences the flow in the outboard sections of the blades which have a relatively small effect on the accumulative rotor aerodynamic torque and blade root bending moments and therefore the selected input data channels. In this study the estimator performance is seen to decrease as the nondimensional wake position magnitude is below ~0.2.

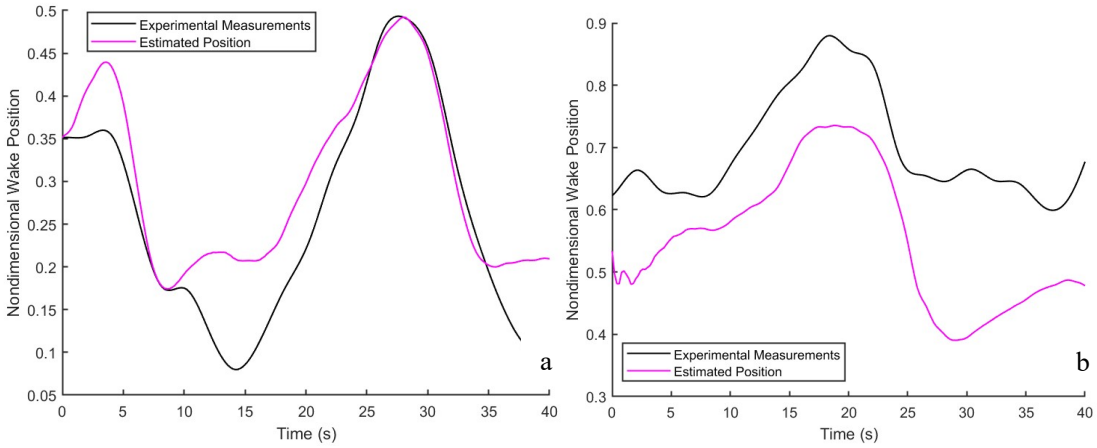

Figure 4: Example validation performance of estimator on wake center position for best case scenarios (a) and worst-case scenarios (b)

4.2 Validation on Medium Fidelity Wind-Farm Simulator

To assess the performance of the methodology using simulated wind turbine data and provide the groundwork for simulator use in further studies, a similar approach for wake estimation model training and validation is performed. In contrast to the routine used for the experimental data, six 10-minute bins are used for training and three 10-minute bins are used for validation. Additionally, the edgewise blade load is included as an input channel and the filtering is no longer employed on the flap-wise blade loads. The reasoning behind the change in channels is due to difficulties in training the wake position estimator using identical settings to those determined using experimental data. Further analysis is required to fully determine the underlying causes driving this discrepancy. An initial hypothesis for the discrepancies is a potential lack of proper induction modelling at the downstream turbine rotor plane in the DWM model especially in partially waked conditions. This modelling deficiency may result in downstream turbine loading and dynamics that are intrinsically different than what is observed in the experimental setup and therefore requires the use of a different set of inputs and outputs for sufficient estimator performance. The following simulated cases are performed under these conditions.

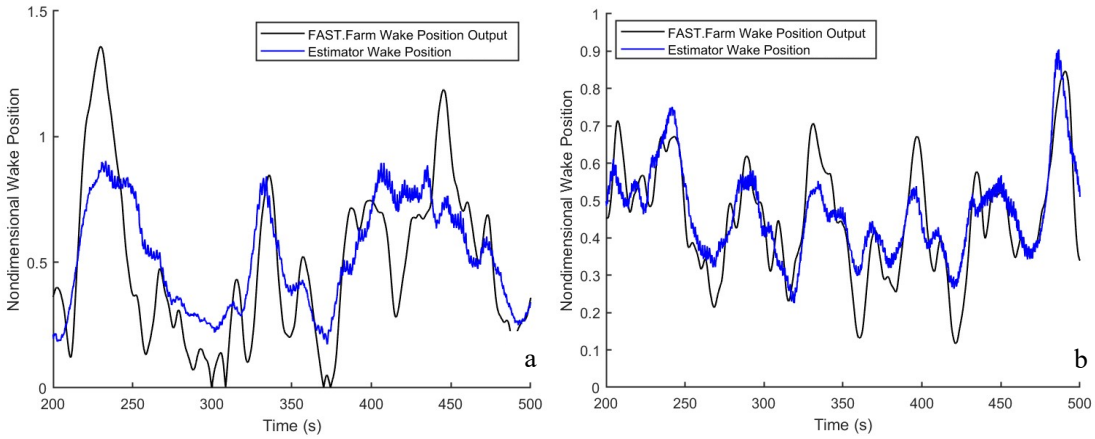

Figure 5: Validation performance of estimator on simulated wind farm data; (Inflow wind speed = 6.7 m/s & TI = 12.6% (a); Inflow wind speed = 8.7 m/s & TI 6% (b))

In Figure 5 validation performance of the wake position estimator using simulation wind turbine and wake position data are shown. The conditions showcased are representative of a low wind speed/high turbulence Figure 5a and a medium wind speed/low turbulence (Figure 5b) flow field. Of significant importance in these results is the wake position estimator's ability to provide sufficiently accurate wake center estimates while operating in close-loop for an extended period of time. This result can be viewed as an extension of the performance the estimator demonstrated on the significantly smaller experimental bins.

In comparing the two validation data bins in Figure 5, the influence of turbulence and wake position magnitude on the wake position estimator becomes apparent. In Figure 5b, all nondimensional wake center positions are well bounded between 0.1 and 1 and the overall wake dynamics is moderate due to the relatively low turbulence intensity of this bin. This type of scenario provides a best-case situation for the wake position estimator as the wake is having maximal influence on the selected data channels. This strong influence is due to the wake moving within a range of locations that allows for significant portions of the rotor blade to operate in waked and freestream conditions during each rotation resulting in significant dynamics in the selected input channels. In contrast, Figure 5a showcases fast wake center position movements along with significant periods of the nondimensional wake position being below 0.2 and above 1. Estimator performance reduction in these cases is consistent with the observations made with experimental data. As an inverse to the near fully waked I/O insensitivity previously discussed, high wake position magnitudes have relatively weak influence on the selected data channels

due to the rotor blades operating in near freestream conditions and therefore relatively small variations in the selected data channels will occur as the magnitude becomes exceedingly large.

4.3 Sensitivity of Wake Position Estimation to Atmospheric Boundary Layer Conditions

To understand the effects of variations in the atmospheric veer rate on wake position estimator performance a parametric study is conducted using the FAST.Farm model of the SWiFT site. The study utilizes estimators trained using FAST.Farm simulated data of the downstream turbine in TurbSim generated flow fields designed with 0 °/m veer rates. These estimators are then given data from FAST.Farm simulations of the downstream wind turbine using TurbSim flow fields identical in all parameters besides the mean wind profile veer rate. The veer rates in this testing set vary from -0.3704 to 0.5556 °/m which results in total veers across the rotor plane of -10° to 15° respectively. The veer profile is designed to be at 0° veer at the rotor hub.

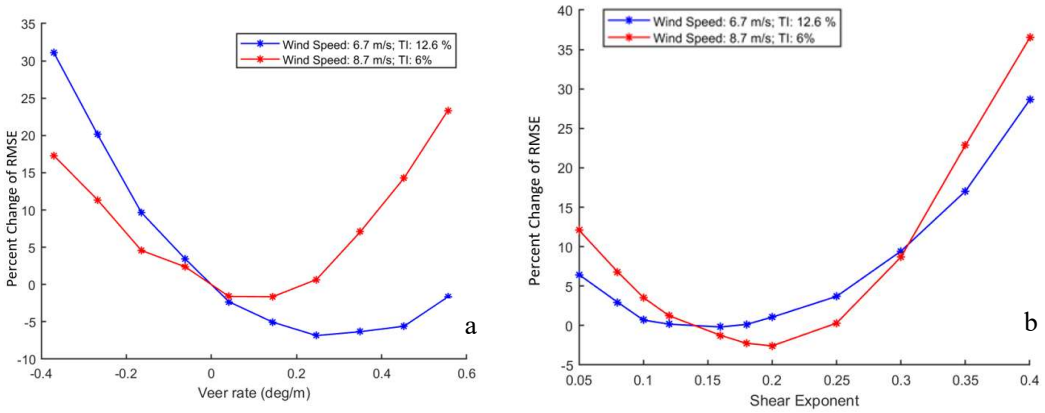

Figure 6: Effect of veer rate (a) and shear exponential (b) on the percent change of the wake position estimator RMSE with respect to the interpolation estimated RMSE at 0 °/m veer rate & 0.14 shear exponential respectively

To quantify the effects of veer on the wake position estimation performance, the percent change of the wake position estimator RMSE for a given test case with respect to interpolation estimated RMSE of the estimator at 0 °/m veer rate is used. This measure is useful in determining the expected percent change in the RMSE of the wake position estimator for a given change in flow field veer rate. From Figure 6a the effects of veer rate on this metric are showcased. It can be observed that there is a parabolic variation in the percent change of the RMSE as veer rate increases for both wind speed and turbulence intensity combinations. For the 8.7 m/s cases, a moderate variation of veer from ~-0.25 to ~0.45 °/m results in a maximum RMSE percent change of 10%. This can be interpreted as the anticipated performance decrease of the estimator in terms of RMSE. In the context of the experimental results, this result translates to an anticipated maximum increase in nondimensional and dimensional wake position RMSE of 0.132 and 0.352 m respectively in the veer rate range of ~-0.25 to ~0.45 °/m. It is noted that in the flow fields generated for the 6.7 m/s parametric study, increasing veer rates reduced the magnitude of maximum wake center position allowing for better estimator performance at increasing veer rates up to 0.247 °/m veer rate. It's currently assumed that using a large number of turbulent flow fields generated with identical settings and different random seeds would produce a parabolic curve centered at the interpolated estimate of the RMSE at 0 °/m veer rate.

A nearly identical parametric study as conducted for the veer rate is conducted for the atmospheric shear exponent to understand the effects of atmospheric shear variation on wake position estimator performance. The TurbSim flow fields used in training the wake position estimator use a shear exponential of 0.14. These estimators are then given output data from FAST.Farm simulations using

TurbSim flow field data identical in all parameters except for the mean wind profile shear exponent. The shear exponents used in this study vary from 0.05 to 0.4. All training and testing data are designed with 0 °/m veer rate.

The effects of the shear exponential are quantified using the same metric as described in the veer study albeit with respect to the interpolated estimate of the RMSE corresponding to a 0.14 shear exponent. Figure 6b showcases the results of this study. It can be seen the variation of the percent change of the RMSE with respect to variations in shear exponential is also parabolic. In addition, the absolute value of the percent change in RMSE is observed to be on the same order of the results in the veer study. Overall, the conclusion can be suggested that variations in the shear exponents of the flow field will introduce minimal performance variation of the wake position estimator over a large range of shear exponents for this relatively small wind turbine. In the context of large-scale turbines however, the shear and veer rates would possess stronger influences on estimator error due to the increased absolute variation in the flow across the rotor plane.

5. Discussion

5.1 Merit of Wake State Estimation in Turbine Operation

Using the proposed estimator, a higher level of situational awareness is available for turbine operators and control engineers allowing for optimization of turbine operation in various waked states. To showcase this potential a parametric study is performed using the FAST.Farm simulation environment and the SWIFT site model. Of interest is the sensitivity and functional relationship of the downwind turbine power with respect to changes in the generator torque constant under various waked conditions. The wake condition is varied by varying the lateral flow field propagation direction while maintaining a nominally 0 degree yaw offset for the leading and trailing turbines. Uniform flow fields are used to avoid the stochastic nature of turbulence and its influence on the turbine. With this procedure, the sensitivities and relationships produced can provide control engineers idealistic guidelines for generator torque variations based on the current waking condition.

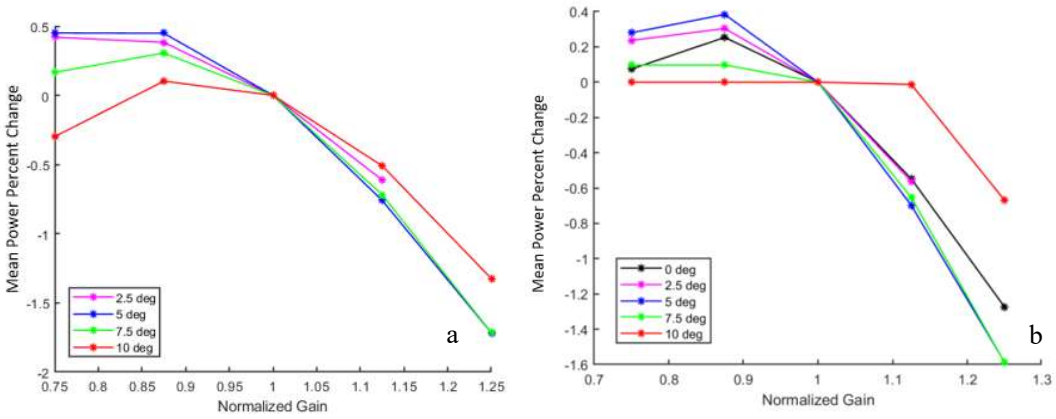

Figure 7: Variation in mean power percent change with respect to generator torque constant for 6.7 m/s (a) & 8.7 m/s (b) uniform inflows and varied inflow angles.

In Figure 7 the resulting relationship between the mean power percent change and the normalized generator torque controller gain constant is shown for wind speeds of 6.7 and 8.7 m/s and a shear exponential of 0.14 at varying flow field propagation angles. In both wind speed scenarios, the standard generator torque constant optimized for undisturbed nonturbulent flow is no longer optimal under waked conditions. By reducing the generator torque constant and allowing the wind turbine to move to a higher tip speed ratio a power performance increase of nearly 0.5% and 0.4% are observed for specific inflow

conditions in each scenario. Preliminary analysis suggests this variation in optimal generator torque constant is a result of the wake changing the lift distribution on the blades and effectively changing the blade design. These results showcase the potential of active wake position-based generator torque control for power optimization using the wake position estimator showcased in this work.

6. Conclusions

In the presented work a novel methodology for estimating the absolute lateral position of a wake center on a downstream turbine using an inverse dynamics approach is introduced. The utilization of RNNs for the purpose of modelling the inverse dynamic relationship allows for an easily obtainable inverse model for a complex system that otherwise would be exhaustively difficult if not impossible to obtain using first principles alone. The showcased results of the methodology show promise in delivering an approach that may be used to provide valuable information to future wind turbine and wind farm control approaches.

Based on the presented results, future work will consist of improving key areas of deficiencies in the observed methodology. Improvements in the robustness of the methodology in situations where the dynamic coupling between the selected I/O data channels are weak (i.e. constant wake position, varying inflow velocity) as well as refinements in the RNN hyperparameters and architecture will be of significant focus. Additionally, the diagnosis of the modelling deficiencies that drive the need for differing I/O channels and settings will provide a better scope of where simulations can be used in developing advanced controllers for use in experimental setups.

Acknowledgments:

This research was supported by the Wind Energy Technologies Office of the U.S. Department of Energy (DOE) Office of Energy Efficiency and Renewable Energy. Sandia National Laboratories is a multi-mission laboratory managed and operated by National Technology & Engineering Solutions of Sandia, LLC, a wholly owned subsidiary of Honeywell International Inc., for the U.S. Department of Energy's National Nuclear Security Administration under contract DE-NA0003525. The views expressed in the article do not necessarily represent the views of the U.S. Department of Energy or the United States Government

7. References

[1] Johnson K and Thomas N 2009 Proceedings of the American Control Conference

[2] Herges T G, Maniaci D C, Naughton B T, Mikkelsen T and Sjöholm M 2017 *Journal of Physics: Conference Series* **854**

[3] Bottasso C L, Cacciola S, and Schreiber J 2018 *Renewable Energy* **116** 155

[4] Pedamkar P 2020 Perceptron Learning Algorithm https://www.educba.com/perceptron-learning- algorithm/

[5] Bitzer T and Omlin 2000 Neural Networks for Chaotic Time Series Prediction.

[6] MATLAB Optimization and Neural Network Toolbox Release 2020b, The MathWorks, Inc., Natick, Massachusetts, United States

[7] Berg J, Bryant J, LeBlanc B, Maniaci D C, Naughton B, Paquette J A, Resor B R, White J and Kroeker D 2014 *AIAA SciTech 32nd Wind Energy Symposium*

[8] White J R, Ennis B L and Herges T G 2018 *AIAA SciTech Wind Energy Symposium*

[9] Jonkman, J and Shaler K 2021 FAST.Farm User's Guide and Theory Manual. Golden, CO: National Renewable Energy Laboratory. NREL/TP-5000-78785.

[10] Jonkman J, Doubrawa P, Hamilton N, Annoni J and Fleming P 2018 *IOP Conf. Series: Journal of Physics: Conf. Series* **1037**

[11] Kelley C and White J 2018 "An Update to the SWiFT V27 Reference Model" Albuquerque, NM: Sandia National Laboratories, SAND2018-11893

[12] Doubrawa P, Quon EW, Martinez-Tossas LA and et al. 2020 *Wind Energy* **23** 2027

[13] Jonkman B J and Buhl Jr. M L 2005, "TurbSim User's Guide", Golden, CO: National Renewable Energy Laboratory. NREL/TP-500-36970

[12] Bitzer, T. & Omlin, Christian. (2000). Neural Networks for Chaotic Time Series Prediction.